DATA-GUIDED RANDOM WALKS FOR FINE-STRUCTURED OBJECT SEGMENTATION

Yongchao Gong, Shiming Xiang and Chunhong Pan

National Laboratory of Pattern Recognition, Institute of Automation, Chinese Academy of Sciences
{yongchao.gong, smxiang and chpan}@nlpr.ia.ac.cn

ABSTRACT

Random walks (RW) is a popular technique for object segmentation. Apart from the satisfactory performance in various applications, its most appealing advantage is the computational efficiency. However, RW often fails to produce complete and connected results in fine-structured (FS) object segmentation. To utilize the high efficiency and overcome the drawbacks in tackling FS objects, we develop a novel approach within the RW framework. Specifically, we propose to introduce labeling preference learned from the image data into the RW model to guide the propagation of random walkers. With the help of the guidance, random walkers are more likely to propagate correctly to the FS regions, thus yielding more accurate results. Similar to RW, this approach also bears properties such as computational efficiency, closed-form solution and unique global optimum. Moreover, it has the capacities of handling disconnected objects and transferring segmentation. Comparative experimental results demonstrate that the proposed approach achieves the state-of-the-art performance in FS object segmentation, with a low requirement of runtime.

Index Terms— Random walks, data-guided random walks, fine-structured object segmentation, labeling preference

1. INTRODUCTION

Object segmentation is an important problem in image processing and understanding. During the past decades, a variety of thoughtful approaches have been developed [1–6]. In many cases, they can produce satisfactory results, but they often fail to handle fine-structured (FS) objects due to the thin and elongated object structures. This drawback prevents these approaches from taking effects in practical applications such as image synthesis and plant modeling. Therefore, FS object segmentation remains a challenging task.

Approaches for object segmentation can be roughly categorized into two groups. One consists of classical approaches based on basic techniques, *e.g.*, graph cuts [2] and random walks [4], and the other includes the variants of these basic techniques.

Graph cuts (GC) [2] is an effective and efficient technique for object segmentation. It formulates the segmentation task as an inference problem on a pairwise Markov random field (MRF), and global optimum is achieved via min-cut/max-flow algorithm [7]. As GC tends to minimize the length of object boundaries, it does not apply to FS objects, which is known as shrinking bias [8–13]. Random walks (RW) [4] is a typical label propagation based approach. Specifically, for each unlabeled pixel, its label is specified according to the probability of a random walker starting from it to reach a labeled pixel. Despite the weaknesses in tackling FS objects, RW is still crucial for object segmentation due to its reasonable physical explanations, computational efficiency and unique global optimum.

This work was supported by the National Natural Science Foundation of China under Grants 61370039, 61272331 and 61331018, and the Beijing Natural Science Foundation under Grant 4142057.

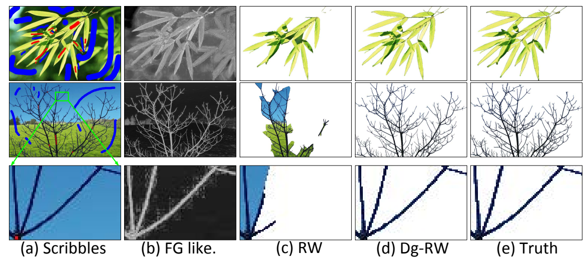

Fig. 1. Illustration of the improvement of introducing guidance into the RW model. (a) Source images with scribbles (red-object, blue-background). (b) Foreground likelihood learned from the seeds specified by the scribbles. (c) Results of RW. (d) Results of the proposed Dg-RW. (e) Ground truth. Images in the last row are the corresponding zoomed-in regions indicated by the green box.

Numerous variants of the basic techniques have been proposed to improve their performance. Among these variants, the ones most relevant to this work are those specially addressing shrinking bias.

To enhance the completeness and connectivity of the segmented FS objects, an intuitive strategy is to introduce certain priors, *e.g.*, connectivity [9], bounding box [14] or tree shape [15], as topological constraints. Unfortunately, incorporating these priors often leads to NP-hardness, thus the optimization procedures are time-consuming and global optima can not be guaranteed. Moreover, as for the approaches in [9, 15], the extra interactions required for each fine part make them impractical for applications.

Another strategy is to develop a more reasonable model. Cooperative graph cuts (CGC) [12] is a typical example. By selectively reweighting the graph edges, the cost of cutting out an FS object with long boundaries is considerably reduced, thus the inherent object structures are more likely to be maintained. As minimizing the energy function of CGC is NP-hard, an iterative strategy is developed to settle for an approximate solution. To achieve the global optimum, this problem is elegantly reformulated as an inference problem in a higher-order MRF [16] called deep random field (DRF) [13]. The performance of this approach is satisfactory, but the model complexity and time required for the exact inference are quite high.

As stated, approaches for FS object segmentation often suffer from high complexities in both models and optimization procedures. In this paper, we propose a simple but effective approach named *data-guided random walks* (Dg-RW). It is developed within the RW framework to utilize its mathematical simplicity and overcome its drawback in segmenting FS objects. For each unlabeled pixel, the probability for its labeling still depends on the propagation of the random walker. More importantly, the propagation is not only based on pairwise connections alone, but also guided by the labeling preference derived from the image data. With the help of the guidance, the random walkers are more likely to propagate correctly to the FS regions, making Dg-RW able to handle FS objects (see Fig. 1). Its effectiveness and efficiency are verified by extensive experiments.

The main advantages of Dg-RW are highlighted as follows:

1. Guidance for the propagation of random walkers is novelly introduced into the RW model. Dg-RW thus largely outperforms RW in FS object segmentation and achieves state-of-the-art performance.

2. Dg-RW bears several notable advantages over existing approaches dealing with FS objects [9, 12–15, 17], namely computational efficiency, closed-form solution and unique global optimum.

3. Dg-RW has other appealing properties, such as handling disconnected objects and transferring segmentation [18]. These properties make Dg-RW more appropriate for practical applications.

2. THE PROPOSED APPROACH

2.1. Notations

Given an image $\mathcal{I}$, the RGB feature vector of pixel i is denoted by $\mathbf{p}_i \in \mathbb{R}^3$. We use $G = (\mathcal{V}, \mathcal{E}, \mathcal{W})$ to denote the weighted graph corresponding to $\mathcal{I}$, where the node set $\mathcal{V}$ corresponds to the pixels in $\mathcal{I}$, the edge set $\mathcal{E}$ contains the pairs of neighboring nodes and each edge $e_{ij} \in \mathcal{E}$ has a weight $w_{ij} \in \mathcal{W}$ that encodes the similarity of neighboring nodes i and j. The seeds specified by the user interactions are denoted by two subsets of $\mathcal{I}$, namely $\mathcal{O}$ and $\mathcal{B}$, with labels $f_O = +1$ and $f_B = -1$ denoting object and background respectively.

2.2. A brief review on random walks

Given the labeled nodes (or user-specified seeds), the goal of RW is to assign each unlabeled node i with label $f_i \in \{f_O, f_B\}$[1] [4]. Specifically, each unlabeled node i is assigned with a probability x_i that a random walker starting from this node first reaches a node labeled f_O on the weighted graph G. The problem of calculating the probabilities of all the nodes, or the vector $\mathbf{x} = \{x_1, x_2, \ldots, x_n\}^{\mathrm{T}}$ (n is the number of pixels in $\mathcal{I}$) is formulated as minimizing the following quadratic energy function with respect to $\mathbf{x}$ [4]:

$$E_{RW}(\mathbf{x}) = \mathbf{x}^{\mathrm{T}}\mathbf{L}\mathbf{x} \ , \tag{1}$$

where $\mathbf{L}$ is the graph Laplacian matrix, defined as $\mathbf{L} = \mathbf{D} - \mathbf{W}$. In matrix $\mathbf{W}$, the (i,j)-th entity is defined as w_{ij} if $e_{ij} \in \mathcal{E}$ or 0 otherwise. Matrix $\mathbf{D}$ is diagonal, with the i-th diagonal entity defined as $d_{ii} = \sum_{j=1}^{n} w_{ij}$. The weight w_{ij} is typically defined as

$$w_{ij} = \exp(-\beta \|\mathbf{p}_i - \mathbf{p}_j\|_2^2) \ , \tag{2}$$

where β is a free positive parameter and $\|\cdot\|_2$ denotes ℓ_2-norm.

For the n nodes in G, we partition them into two subsets, $\mathcal{V}_L$ and $\mathcal{V}_U$ (labeled and unlabeled). Correspondingly, the orders of them in both $\mathbf{L}$ and $\mathbf{x}$ are rearranged so that all the labeled nodes come first. Therefore, $\mathbf{L}$ and $\mathbf{x}$ can be decomposed into block matrices, namely

$$\mathbf{L} = \begin{bmatrix} \mathbf{L}_L & \mathbf{B} \\ \mathbf{B}^{\mathrm{T}} & \mathbf{L}_U \end{bmatrix}, \ \mathbf{x} = \begin{bmatrix} \mathbf{f}_L \\ \mathbf{x}_U \end{bmatrix}, \tag{3}$$

where $\mathbf{f}_L$ contains all the known labels, *i.e.*, for each node $i \in \mathcal{V}_L$,

$$f_i = \begin{cases} f_O, & \text{if node } i \in \mathcal{O} \\ f_B, & \text{if node } i \in \mathcal{B} \ . \end{cases} \tag{4}$$

According to [4], minimizing $E_{RW}(\mathbf{x})$ in Eq. (1) with respect to $\mathbf{x}_U$ is equivalent to solving a sparse system of linear equations:

$$\mathbf{L}_U \mathbf{x}_U = -\mathbf{B}^{\mathrm{T}}\mathbf{f}_L \ . \tag{5}$$

For two-label segmentation problems, each node $i \in \mathcal{V}_U$ is then assigned with a label $f_i = f_O$ if $x_i \geq 0$ or $f_i = f_B$ otherwise.

[1] It is worth noting that RW is originally proposed for simultaneous multi-label segmentation [4], but this work only focuses on two-label, or object/background segmentation, and can be viewed as a particular case of RW.

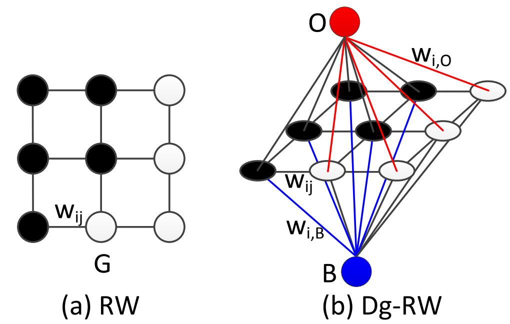

Fig. 2. Graph structures of (a) RW and (b) Dg-RW. On the basis of RW, we additionally add two virtual nodes O (red) and B (blue) to denote object and background respectively. They are fully connected to each node in G and these connections serve as guidance for the propagation of the random walkers. Red/blue connections indicate that the corresponding nodes are assigned as object/background.

2.3. Data-guided random walks

Despite many appealing properties (refer to [4]), RW suffers from several inherent drawbacks. According to [4], in Eq. (5) $\mathbf{L}_U$ is nonsingular only if G is connected, or each connected component of G contains a seed, making RW inappropriate for images with many disconnected objects. Apart from being used as boundary conditions (*i.e.*, $\mathbf{f}_L$) to ensure the nonsingularity of $\mathbf{L}_U$, the seeds have not been fully exploited for other usages. Moreover, since the random walkers are limited to propagate according to only pairwise connections, label information is difficult to reach the FS regions, thus RW often fails to accurately capture the object boundaries and details.

To overcome the drawbacks of RW, we propose a novel approach in the following. We observe that the performance of RW is prone to degrade mainly because only image gradients (refer to Eq. (2)) are used in the propagation of random walkers, while other information is not. For this reason, we propose to incorporate labeling preference into the RW model to guide the propagation. As illustrated in Fig. 2, on the basis of the RW model, we additionally add two virtual nodes O and B to denote object and background, respectively. Each node $i \in \mathcal{V}$ is connected to the two nodes with weights $w_{i,O}$ and $w_{i,B}$ calculated by

$$w_{i,O} = \frac{\log \Pr(\mathbf{p}_i|f_O)}{\log \Pr(\mathbf{p}_i|f_O) + \log \Pr(\mathbf{p}_i|f_B)} \ , \ w_{i,B} = 1 - w_{i,O} \ , \tag{6}$$

where the two probabilities $\Pr(\mathbf{p}_i|f_O)$ and $\Pr(\mathbf{p}_i|f_B)$ are the foreground and background likelihood of node i respectively. Note that the graph structure in Fig. 2(b) is similar to that of GC [2], but they have different explanations[2]. Since the weights indicating the labeling preference are derived from the image data, we name the proposed approach *data-guided random walks* (Dg-RW).

The guidance for node i is then formulated as an energy term

$$E_g(x_i) = w_{i,O}(x_i - f_O)^2 + w_{i,B}(x_i - f_B)^2 \ . \tag{7}$$

For all the nodes in $\mathcal{I}$, the energy terms sum into

$$E_g(\mathbf{x}) = \mathbf{x}^{\mathrm{T}}\mathbf{x} - 2(f_O\mathbf{w}_O + f_B\mathbf{w}_B)^{\mathrm{T}}\mathbf{x} + C_1 \ , \tag{8}$$

where $\mathbf{w}_* = \{w_{1,*}, w_{2,*}, \ldots, w_{n,*}\}^{\mathrm{T}}$ ('$*$' denotes the subscripts 'O' or 'B') and C_1 is a constant independent of $\mathbf{x}$.

By combining the two energy terms in Eq. (1) and Eq. (8) together, we obtain the energy function of Dg-RW, which is

[2] In Dg-RW the two virtual nodes are used to guide the propagation, while in GC they work as the source and sink nodes of the flow network [2].

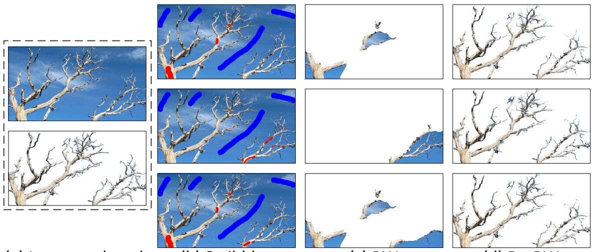

Fig. 3. Comparison of RW and Dg-RW in handling disconnected objects. (a) Source image and ground truth. (b) Scribbles (red-object, blue-background) on a single object (top: left object alone, middle: right object alone) and both objects (bottom). (c) Results of RW. (d) Results of Dg-RW. Note that Dg-RW performs much better than RW in capturing the inherent structures of the disconnected objects.

$$\begin{aligned} E(\mathbf{x}) &= E_{RW}(\mathbf{x}) + \lambda E_g(\mathbf{x}) \\ &= \mathbf{x}^{\mathrm{T}}(\mathbf{L}+\lambda\mathbf{I})\mathbf{x} - 2\lambda(f_O\mathbf{w}_O + f_B\mathbf{w}_B)^{\mathrm{T}}\mathbf{x} + \lambda C_1 \ , \end{aligned} \tag{9}$$

where λ is a positive parameter to indicate the relative importance between the two energy terms and $\mathbf{I}$ is an identity matrix. Let $\widehat{\mathbf{L}} = \mathbf{L}+\lambda\mathbf{I}$, $\widehat{\mathbf{w}} = \lambda(f_O\mathbf{w}_O + f_B\mathbf{w}_B)$ and ignore the constant, we obtain

$$\widehat{E}(\mathbf{x}) = \mathbf{x}^{\mathrm{T}}\widehat{\mathbf{L}}\mathbf{x} - 2\widehat{\mathbf{w}}^{\mathrm{T}}\mathbf{x} \ . \tag{10}$$

Similar to Eq. (3), we decompose $\widehat{\mathbf{L}}$, $\widehat{\mathbf{w}}$ and $\mathbf{x}$ into

$$\widehat{\mathbf{L}} = \begin{bmatrix} \widehat{\mathbf{L}}_L & \widehat{\mathbf{B}} \\ \widehat{\mathbf{B}}^{\mathrm{T}} & \widehat{\mathbf{L}}_U \end{bmatrix}, \ \widehat{\mathbf{w}} = \begin{bmatrix} \widehat{\mathbf{w}}_L \\ \widehat{\mathbf{w}}_U \end{bmatrix}, \ \mathbf{x} = \begin{bmatrix} \mathbf{f}_L \\ \mathbf{x}_U \end{bmatrix}, \tag{11}$$

In this way, Eq. (10) can be rewritten with respect to $\mathbf{x}_U$ as

$$\widehat{E}(\mathbf{x}_U) = \mathbf{x}_U^{\mathrm{T}}\widehat{\mathbf{L}}_U\mathbf{x}_U + 2\mathbf{f}_L^{\mathrm{T}}\widehat{\mathbf{B}}\mathbf{x}_U - 2\widehat{\mathbf{w}}_U^{\mathrm{T}}\mathbf{x}_U + C_2 \ . \tag{12}$$

where C_2 is a constant independent of $\mathbf{x}_U$. Minimizing the quadratic function $\widehat{E}(\mathbf{x}_U)$ with respect to $\mathbf{x}_U$ is equivalent to solving a sparse system of linear equations, with a closed-form solution

$$\widehat{\mathbf{L}}_U\mathbf{x}_U = \widehat{\mathbf{w}}_U - \widehat{\mathbf{B}}^{\mathrm{T}}\mathbf{f}_L \ . \tag{13}$$

As with in RW, we binarize the optimal solution $\mathbf{x}_U^*$ to be $\mathbf{f}_U$, and obtain the final labeling $\mathbf{f} = [\mathbf{f}_L^{\mathrm{T}}, \ \mathbf{f}_U^{\mathrm{T}}]^{\mathrm{T}}$ for the segmentation task.

2.4. Some properties of Dg-RW

Similar to RW, Dg-RW also has the advantages such as computational efficiency, closed-form solution and unique global optimum. Meanwhile, due to the introduction of the guidance, Dg-RW is capable of tackling FS objects. Moreover, in comparison to $\mathbf{L}$, the nonsingularity of $\widehat{\mathbf{L}} = \mathbf{L}+\lambda\mathbf{I}$ is guaranteed and it is unnecessary to require G is connected, or each connected component contains a seed [4]. This yields another two appealing properties of Dg-RW, *e.g.*, handling disconnected objects and transferring segmentation [18].

Fig. 3 illustrates the capacity of Dg-RW in tackling disconnected objects. It is known that RW fails to correctly segment a connected component if it does not contain a seed. This issue has already been addressed in [19], where the approach is designed to reduce the required amount of interactions for images with many disconnected objects, *e.g.*, blood cell images. In our approach, with the help of the guidance, label information is likely to propagate to such components, yielding satisfactory results. This property also shows that Dg-RW is robust to the variations of seed locations.

Transferring segmentation [18] means given an exemplar image with seeds, Dg-RW can segment other images with similar appearances even in absence of seeds. It can be interpreted as follows. The parameters of appearance models are first learned from the exemplar image. Then they are used to calculate the likelihood of the test image to obtain the corresponding weight $\widehat{\mathbf{w}}$. Then $\widehat{E}(\mathbf{x})$ in Eq. (10) is minimized directly with respect to $\mathbf{x}$, yielding a closed-form solution

$$\widehat{\mathbf{L}}\mathbf{x} = \widehat{\mathbf{w}} \ , \tag{14}$$

and the final labeling $\mathbf{f}$ is the binarization of the optimal solution $\mathbf{x}^*$. Fig. 4 demonstrates this property. In Fig. 4(b), we see Dg-RW produces satisfactory results for the test images. Therefore, given an exemplar image, this property enables us to automatically segment similar images without interactions. The interaction burden thus can be largely reduced when segmenting images containing similar contents or captured in similar scenes, or sequential frames in videos.

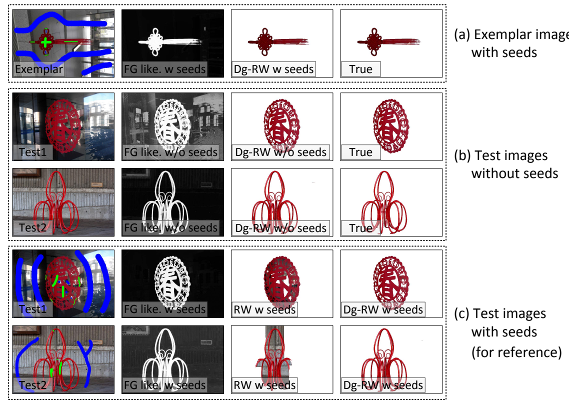

Fig. 4. Demonstration of transferring segmentation using Dg-RW. (a) Exemplar image with seeds (green-object, blue-background). (b) Test images without seeds. (c) Test images with seeds (these results are attached only *for reference*). Note that Dg-RW produces comparable results for the test images both with and without ('w' or 'w/o') seeds. In addition, these results are much better than those of RW, which only works when seeds are provided.

3. EXPERIMENTS

In this section, we apply the proposed Dg-RW to FS object segmentation and make comparisons with several representative approaches.

Data set description. Totally we evaluate on three data sets:

1. 'Twigs&Legs' data set [12,20], a challenging data set containing 16 images for evaluating FS object segmentation approaches.

2. 'FS100' data set, our own collection, consisting of 100 images involving various FS objects, with hand-labeled ground truth.

3. 'Grabcut' data set [3,21], a benchmark for image segmentation containing 50 images, with the default trimaps as interactions. This data set is used to verify that Dg-RW can also handle relatively compact objects and complex backgrounds.

Evaluation criteria. We use two criteria for the evaluations:

Intersection-over-union score (*IOU*) [22]: the area of the intersection of the segmented object mask and the ground truth object mask divided by the area of their union.

Error rate (*ERROR*) [12]: the number of incorrectly labeled pixels divided by the total number of pixels in the image.

Approaches for comparisons. We compare *six* approaches with Dg-RW. Random walks (RW) [4] is the baseline. Graph cuts (GC) [2] and Laplacian coordinates (LC) [6] are two powerful and efficient basic techniques, and LC is also a label propagation based approach. Geodesic star convexity (GSC) [11], cooperative graph cuts (CGC) [12] and deep random field (DRF) [13] are specially developed to tackle FS objects, and DRF is the state-of-the-art

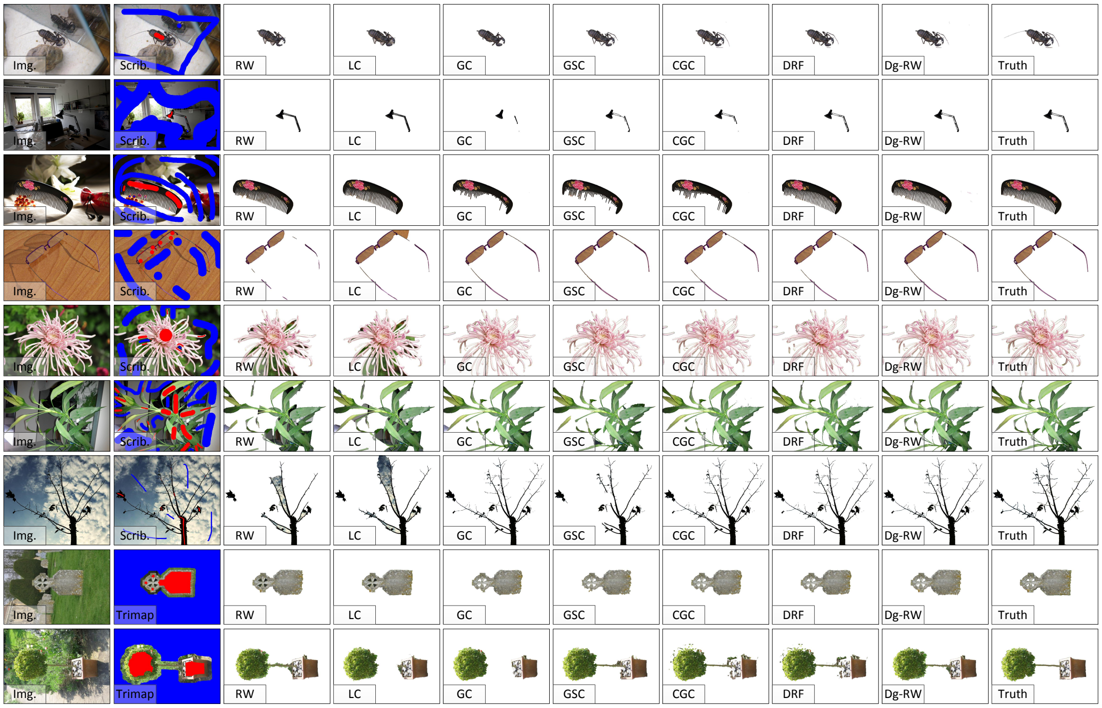

Fig. 5. Qualitative results of nine images from 'Twigs&Legs', 'FS100' and 'Grabcut' data sets. Each row corresponds to one image from the three data sets. In each row, from left to right are source image, scribbles or trimap (red-object, blue-background), results of RW, LC, GC, GSC, CGC, DRF and Dg-RW, and ground truth. Due to the space limitation, please zoom in the images for the details.

Table 1. Quantitative comparisons of the seven approaches. All the results listed here are averaged on all the images in each of the three data sets. The IOUs and ERRORs in red indicate the best and blue the second best. Best viewed in color.

Data sets	Criteria	RW	LC	GC	GSC	CGC	DRF	Dg-RW
Twigs&Legs	IOU (%)	68.8813	65.0474	73.8629	73.1072	77.7556	79.9500	79.8411
	ERROR (%)	4.9439	6.6369	1.4413	1.4847	0.9858	0.8875	0.9043
FS100	IOU (%)	76.8536	74.9332	87.7275	85.5719	88.7020	89.4986	89.4164
	ERROR (%)	5.6966	6.2953	2.0267	2.7132	1.8768	1.7657	1.7397
Grabcut	IOU (%)	91.5424	92.6499	92.5849	92.7446	92.5904	92.6877	93.2777
	ERROR (%)	1.1075	0.8695	0.9428	0.9121	0.9381	0.9091	0.7825

approach. For these six approaches, we use the publicly available codes [23–29] provided by the authors and tune the parameters to achieve the overall best performance on each data set. To calculate the foreground and background likelihood for Dg-RW (see Eq. (6)), as well as GC, GSC, CGC and DRF, we fit two Gaussian mixture models each with five components to the seeds [3, 9, 12, 13]. In Dg-RW, we adopt an 8-neighbor graph structure and uniformly set $\beta = 85$ and $\lambda = 0.001$ for all the three data sets.

Qualitative comparisons. Qualitative comparisons of the results on two images from 'Twigs&Legs', five from 'FS100' and two from 'Grabcut' are shown in Fig. 5. It can be seen that Dg-RW achieves better or comparable performance, with complete and connected segmented objects and accurate object boundaries and details.

Quantitative comparisons. The *IOU* and *ERROR* averaged on all the images in each data set are listed in Table 1. Although Dg-RW is slightly inferior to the state-of-the-art approach DRF in some cases, *e.g.*, on 'Twigs&Legs', their overall performance is comparable and Dg-RW also outperforms all the other approaches. Particularly, the large improvement over RW verifies the effectiveness of introducing the guidance. Moreover, it can be concluded from the performance on 'Grabcut' that Dg-RW is also capable of handling compact objects and complex backgrounds. On the other hand, efficiency is also a main concern about Dg-RW. For the seven approaches listed in Table 1, their averaged runtime is 1.28s, 2.43s, 0.61s, 1.07s, 31.60s, 41.09s and 1.85s, respectively. Obviously, Dg-RW is a quite efficient approach in comparison to other ones dealing with FS objects, namely CGC and DRF.

4. CONCLUSION

In this paper, we presented a novel *data-guided random walks* approach for the challenging task of fine-structured object segmentation. In this approach, labeling preference is introduced into the RW model, with the purpose of effectively guiding the the propagation of random walkers. The random walkers are thus more likely to propagate correctly to the fine-structured regions. This approach bears several appealing properties, such as computational efficiency, closed-form solution, unique global optimum, as well as the capacities of handling disconnected objects and transferring segmentation. Comparative experiments demonstrate that the proposed approach is effective to tackle fine-structured objects and achieves the state-of-the-art performance with a low requirement of runtime.

5. REFERENCES

[1] Tony F. Chan and Luminita A. Vese, "Active contours without edges," *IEEE Trans. Image Process.*, vol. 10, no. 2, pp. 266–277, 2001.

[2] Yuri Boykov and Marie-Pierre Jolly, "Interactive graph cuts for optimal boundary and region segmentation of objects in N-D images," in *Proc. IEEE Int. Conf. Comput. Vis.*, 2001, pp. 105–112.

[3] Carsten Rother, Vladimir Kolmogorov, and Andrew Blake, ""GrabCut"–interactive foreground extraction using iterated graph cuts," in *Proc. ACM SIGGRAPH*, 2004, pp. 309–314.

[4] Leo Grady, "Random walks for image segmentation," *IEEE Trans. Pattern Anal. Mach. Intell.*, vol. 28, no. 11, pp. 1768–1783, 2006.

[5] Shiming Xiang, Feiping Nie, Chunxia Zhang, and Changshui Zhang, "Interactive natural image segmentation via spline regression," *IEEE Trans. Image Process.*, vol. 18, no. 7, pp. 1623–1632, 2009.

[6] Wallace Casaca, Luis Gustavo Nonato, and Gabriel Taubin, "Laplacian coordinates for seeded image segmentation," in *Proc. IEEE Int. Conf. Comput. Vis. Pattern Recognit.*, 2014, pp. 384–391.

[7] Yuri Boykov and Vladimir Kolmogorov, "An experimental comparison of min-cut/max-flow algorithms for energy minimization in vision," *IEEE Trans. Pattern Anal. Mach. Intell.*, vol. 26, no. 9, pp. 1124–1137, 2004.

[8] Vladimir Kolmogorov and Yuri Boykov, "What metrics can be approximated by geo-cuts, or global optimization of length/area and flux," in *Proc. IEEE Int. Conf. Comput. Vis.*, 2005, pp. 564–571.

[9] Sara Vicente, Vladimir Kolmogorov, and Carsten Rother, "Graph cut based image segmentation with connectivity priors," in *Proc. IEEE Int. Conf. Comput. Vis. Pattern Recognit.*, 2008, pp. 1–8.

[10] Brian L. Price, Bryan S. Morse, and Scott Cohen, "Geodesic graph cut for interactive image segmentation," in *Proc. IEEE Int. Conf. Comput. Vis. Pattern Recognit.*, 2010, pp. 3161–3168.

[11] Varun Gulshan, Carsten Rother, Antonio Criminisi, Andrew Blake, and Andrew Zisserman, "Geodesic star convexity for interactive image segmentation," in *Proc. IEEE Int. Conf. Comput. Vis. Pattern Recognit.*, 2010, pp. 3129–3136.

[12] Stefanie Jegelka and Jeff Bilmes, "Submodularity beyond submodular energies: Coupling edges in graph cuts," in *Proc. IEEE Int. Conf. Comput. Vis. Pattern Recognit.*, 2011, pp. 1897–1904.

[13] Pushmeet Kohli, Anton Osokin, and Stefanie Jegelka, "A principled deep random field model for image segmentation," in *Proc. IEEE Int. Conf. Comput. Vis. Pattern Recognit.*, 2013, pp. 1971–1978.

[14] Victor S. Lempitsky, Pushmeet Kohli, Carsten Rother, and Toby Sharp, "Image segmentation with a bounding box prior," in *Proc. IEEE Int. Conf. Comput. Vis.*, 2009, pp. 277–284.

[15] Jan Stühmer, Peter Schröder, and Daniel Cremers, "Tree shape priors with connectivity constraints using convex relaxation on general graphs," in *Proc. IEEE Int. Conf. Comput. Vis.*, 2013, pp. 2336–2343.

[16] Pushmeet Kohli, Lubor Ladicky, and Philip H. S. Torr, "Robust higher order potentials for enforcing label consistency," *Int. J. Comput. Vis.*, vol. 82, no. 3, pp. 302–324, 2009.

[17] Petter Strandmark, Johannes Ulén, Fredrik Kahl, and Leo Grady, "Shortest paths with curvature and torsion," in *Proc. IEEE Int. Conf. Comput. Vis.*, 2013, pp. 2024–2031.

[18] Shuangshuang Li, Yonghao He, Shiming Xiang, LingFeng Wang, and Chunhong Pan, "Transferring segmentation from image to image via contextual sparse representation," in *Chinese Conf. Pattern Recognit.*, 2014, pp. 1–11.

[19] Leo Grady, "Multilabel random walker image segmentation using prior models," in *Proc. IEEE Int. Conf. Comput. Vis. Pattern Recognit.*, 2005, pp. 763–770.

[20] Stefanie Jegelka and Jeff Bilmes, "'Twigs&Legs' data set," `http://melodi.ee.washington.edu/~jegelka/cc/index.html`.

[21] Carsten Rother, Vladimir Kolmogorov, and Andrew Blake, "'GrabCut' data set," `http://research.microsoft.com/en-us/um/cambridge/projects/visionimagevideoediting/segmentation/grabcut.htm`.

[22] PASCAL Visual Object Classes Challenge 2009 (VOC2009), ," `http://host.robots.ox.ac.uk/pascal/VOC/voc2009/`.

[23] Leo Grady, "Random walker," `http://cns.bu.edu/~lgrady/software.html`.

[24] Wallace Casaca, Luis Gustavo Nonato, and Gabriel Taubin, "Laplacian coordinates for seeded image segmentation," `http://sites.google.com/site/wallacecoc/publications`.

[25] Vladimir Kolmogorov, "Max-flow/min-cut library," `http://vision.csd.uwo.ca/code/`.

[26] Varun Gulshan, "Geodesic star convexity," `http://www.robots.ox.ac.uk/~vgg/research/iseg/`.

[27] Evan Shelhamer, "Cooperative cuts," `http://coopcut.berkeleyvision.org`.

[28] Pushmeet Kohli and Philip H. S. Torr, "Effciently solving dynamic markov random fields using graph cuts," in *Proc. IEEE Int. Conf. Comput. Vis.*, 2005, pp. 922–929.

[29] Anton Osokin, "Code for the algorithms of cooperative cuts," `http://research.microsoft.com/en-us/um/people/pkohli/code/coopCuts_CVPR2013.zip`.